HHS Public Access

Author manuscript

Exp Eye Res. Author manuscript; available in PMC 2021 February 22.

Published in final edited form as:

Exp Eye Res. 2020 October ; 199: 108168. doi:10.1016/j.exer.2020.108168.

In vivo immune cell dynamics in the human cornea

Luisa H. Colorado[a,*], **Katie Edwards**[a], **Holly R. Chinnery**[b], **Haydee E. Bazan**[c]

[a]Institute of Health and Biomedical Innovation, School of Optometry and Vision Science, Queensland University of Technology, Kelvin Grove, QLD, 4069, Australia

[b]Department of Optometry and Vision Sciences, The University of Melbourne, Parkville, VIC, 3052, Australia

[c]Department of Ophthalmology and Neuroscience Center of Excellence, School of Medicine, Louisiana State University Health New Orleans, 2020 Gravier St., Suite D, New Orleans, LA, 70112, USA

Abstract

In vivo confocal microscopy (IVCM) allows the evaluation of the living human cornea at the cellular level. The non-invasive nature of this technique longitudinal, repeated examinations of the same tissue over time. Image analysis of two-dimensional time-lapse sequences of presumed immune cells with and without visible dendrites at the corneal sub-basal nerve plexus in the eyes of healthy individuals was performed. We demonstrated evidence that cells without visible dendrites are highly dynamic and move rapidly in the axial directions. A number of dynamic cells were observed and measured from three eyes of different individuals. The total average displacement and trajectory speeds of three cells without visible dendrites (N = 9) was calculated to be 1.12 ±0.21 and 1.35 ± 0.17 μm per minute, respectively. One cell with visible dendrites per cornea was also analysed. Tracking dendritic cell dynamics in vivo has the potential to significantly advance the understanding of the human immune adaptive and innate systems. The ability to observe and quantify migration rates of immune cells in vivo is likely to reveal previously unknown insights into corneal and general pathophysiology and may serve as an effective indicator of cellular responses to intervention therapies.

Keywords

Corneal dendritic cells; Corneal immune cells; Cells without visible dendrites; Cells with visible dendrites; In vivo confocal microscopy

[*]Corresponding author. Institute of Health and Biomedical Innovation, Queensland University of Technology, 60 Musk Avenue, Room Q-504, Level 5, Kelvin Grove, Queensland, 4059, Australia. luisa.holguincolorado@qut.edu.au (L.H. Colorado). .

Author contributions

LHC: Conceived and designed the analysis; Collected the data; Contributed data or analysis tools; Performed the analysis; Wrote the paper.

KE: Designed the analysis; Collected the data; Contributed data or analysis tools.

HC: Contributed data or analysis tools.

HB: Contributed data or analysis tools.

Declaration of competing interest

The authors declare that they have no conflicts of interest.

Appendix A. Supplementary data

Supplementary data to this article can be found online at https://doi.org/10.1016/j.exer.2020.108168.

1. Introduction

In the healthy human, the presence of resident dendritic cells (DCs) has been confirmed in the corneal epithelium, with a higher number residing in the peripheral area compared to the center (Zhivov et al., 2005). Upon corneal infection, an increased number of DCs has been reported in central and peripheral cornea concomitant with morphological changes such as increased size and elongation of dendrites (Mastropasqua et al., 2006).

Research in mice suggests that the paucity of resident DCs in the central cornea is thought to support immune privilege (Niederkorn., 1990), as explained by higher transplant success upon transfer of grafts with low numbers of “passenger” DCs, which reduces the likelihood of triggering a graft-destroying adaptive immune response (Williams and Coster., 1997). In addition to their presumed role as professional antigen presenting cells, evidence from mouse studies suggest that corneal DCs dynamically perform immune surveillance of the corneal epithelium by retracting and extending their dendrites (Lee et al., 2010; Ward et al., 2007). Furthermore, in vivo studies in mouse models have demonstrated that DCs increase migration speed under inflammatory conditions (Lee et al., 2010; Seyed-Razavi et al., 2019; Ward et al., 2007). Despite the relative ease of acquiring static in vivo images of DCs in humans, dynamic corneal DC behavior has never been reported in living human eyes.

In humans, in vivo confocal microscopy (IVCM) has been used to describe the morphological and cell density changes of epithelial DCs in local and systemic conditions (Alzahrani et al., 2016; Mastropasqua et al., 2006; Rosenberg et al., 2002; Su et al., 2006; Zhivov et al., 2005), with an increased number of DCs with elongated processes reported in both non-Sjogren’s and Sjogren’s syndrome dry eye disease (Machetta et al., 2014). More recent studies have also proposed a grading scale where the morphology of corneal DCs has been included as an indication of the inflammatory state of the cornea. This scale suggests that healthy corneas predominantly display DC bodies without dendrites while in diseased inflammatory corneas the cell bodies include long processes (Choi et al., 2017; Marsovszky et al., 2013). Thus, while the unstained cells visible by IVCM in healthy humans could, in theory, be any phenotype, the morphology, and lack of dendrites, suggest that these cells are likely immature dendritic cells (Cruzat et al., 2011; Hamrah et al., 2002).

Recent animal work using corneal explants suggest that during wound healing of bovine corneas, bone marrow-derived cells from the stroma move at a displacement speed (distance from start to end point) of around 0.18 μm/min and an average trajectory speed (migratory path) of 0.83 μm/min. These same parameters increased dramatically when cells were isolated from their niche in a planar culture dish (4.28 and 7.45 μm/min, respectively) (Zhao et al., 2003). The difference in these findings suggests that these dynamic cells behave differently depending on their environmental conditions. This study also provided evidence that cells with dendrites moved within and between focal planes (Zhao et al., 2003), indicating that these cells travel in X, Y, Z directions throughout the corneal stroma, in the absence of the epithelium, during wound healing. In contrast, another study suggests that isolated dendritic shaped cells from the cultured human stroma move in a centripetal manner

in serum-containing media as observed with time-lapse differential interference contrast imaging (Lin et al., 2010).

There is little evidence of corneal dendritic and other immune cell behavior in vivo, as the methodology to study in situ “time-lapse” cell dynamics in animal and cadaveric human eyes are mostly ex vivo, and have only recently been developed (Seyed-Razavi et al., 2013; Steven et al., 2011; Zhou and Petroll, 2010; Lee et al., 2010). Most investigations with IVCM have visualized a variety of cell types and neural structures in the human living cornea at a single time point (Patel and McGhee, 2007; Tavakoli et al., 2008; Villani et al., 2014). However, the opportunity to non-invasively perform repeated imaging over time allows observation of in-vivo immune cell dynamics in human corneas. There are other established methods for visualising cellular dynamics in human organs such as lymph nodes and skin. However, these techniques requires biopsy samples and are relatively invasive and non-repeatable.

This novel observational report illustrates for the first time dynamic immune cell kinetics using “time-lapse” imaging of 12 cells in the corneas of three healthy individuals. Cell displacement and trajectory speeds, as well as directional persistence ratio and cell area in at least three cells without visible dendrites and one without visible dendrites of each cornea over a short time-period was calculated.

2. Material and methods

2.1. Study design and participants

The study was approved by the Queensland University of Technology, Human Research Ethics Committee and was conducted in accor-dance with the tenets of the Declaration of Helsinki.

This was an exploratory, observational investigation. The three volunteers were females between 21 and 41 years of age and at the time of enrollment had no history of contact lens wear, current pregnancy, ocular trauma or surgery, ocular surface dysfunction, current or long-term use of topical ocular medication, or ocular or systemic disease that may affect the ocular surface.

After written informed consent was obtained from the participants, the ocular surface integrity was examined using the slit-lamp bio-microscope, yellow observation filter; fluorescein-impregnated strip and Efron grading scale (Efron, 1998) for corneal staining. Grading scores under 2 scale-points were required before IVCM.

2.2. In vivo corneal confocal microscopy

The Heidelberg Retina Tomograph 3 (HRT3) with Rostock Cornea Module (Heidelberg Engineering, Germany) was used. The microscope operates by scanning a laser beam spot of less than 1 μm in diameter sequentially over each point of the examined area. This instrument has a field of view of 400 μm × 400 μm using a fixed 63X objective lens that has a numerical aperture of 0.9. It uses a 670 nm red wavelength Helium–Neon diode laser as the illumination source. This is a class 1 laser system and therefore does not pose any ocular

safety hazard; however, the manufacturer recommends a maximum period of exposure of 45 min in a single examination period.

2.3. Examination procedure

To prevent blinking and patient discomfort during image acquisition, local anesthetic (benoxinate hydrochloride 0.4%, Chauvin, France) was applied to the cornea. The contact duration time between the ocular surface and the front lens of the microscope, the Tomocap™, did not exceed 5 min per session and a single drop of anesthetic was required on four separate occasions during the entire 50-min examination, by approximately 12 min apart or when the participant reported corneal sensitivity at the time of contact. A minimum of 33 images of the same location from the central cornea were captured at the same depths in X and Y direction using the sequence mode of the Heidelberg Program. A large drop of GenTeal Gel (carbomer 940, Ciba Vision Ophthalmics) was applied onto the tip of the lens, then the Tomocap™ was placed over the objective lens.

The head of the participant was placed in the head and chin rest, and the participant was instructed to look straight ahead and gaze at the target located on the wall. The target was aligned to the central corneal red reflex of laser projected in the center of the pupil (Fig. 1).

2.4. Imaging strategy

As obtaining the same field of view repeatedly over time using IVCM is challenging, an imaging strategy was developed by identifying the centre of the cornea based on the alignment of nerve fibers (vertical orientation) and the geographical position relative to the sub-basal nerve plexus whorl. The whorl of the sub-basal nerve plexus in the inferocentral cornea is a reliable, stationary landmark during imaging due to its unique location. Therefore, the fixation target of the IVCM was manually aligned for each participant with the central corneal reflex while capturing images immediately after identifying nerve fibres in vertical direction located upper the sub-basal nerve plexus whorl (Fig. 1A).

2.5. Image analysis

Tracking cell movement was made possible by using neighboring nerve junctions as stationary landmarks relative to the center of the cell body. A custom-written software program, previously used to measure corneal nerve migration rate, was used (Edwards et al., 2016). Corneal nerve fibres have a minimal migration rate of approximately 0.004 μm/min (Al Rashah et al., 2018) and therefore nerve landmarks were relatively static landmarks against which the movement of a given migrating cell was measured. As part of the image analysis a nerve junction in each selected image was used as a control in order to explore the accuracy and variability of the measurement technique.

Images with repeatable and re-identifiable corneal nerve landmarks were chosen for analysis. The image selected for each session needed to include the in-focus area of interest, at approximately the same depth in order to measure cell displacement, trajectory and persistence. About 3% of images were successfully included in the time-lapse analysis and at least three cells without visible dendrites and one with visible dendrites per session were able to be tracked within the overlapped images selected for each session in the right eye of

three different subjects. To create short time-lapse videos, images sequences were registered using the 'Register Virtual Stack' Plugin in FIJI/ImageJ.

The cell area was measured using the area selection tools of the ImageJ software (Schneider et al., 2012). The trajectory speed was calculated as the total length traveled by the cells divided by time; displacement speed was calculated as the straight-line distance between the start and end positions of a cell divided by time and migration efficiency (persistence) was calculated as the ratio of displacement speed and trajectory speed, which indicates how persistent a cell moves in one direction at a given time (Beltman et al., 2009).

3. Results

3.1. Participant characteristics

Corneas of three female participants of 25, 35 and 41 years of were examined using the Efron scales (Efron, 1998). Corneal was graded as 0.5 ± 0.3 points and ocular surface integrity was markable prior to in vivo imaging.

3.2. In vivo confocal microscopy

A total area of approximately 650 × 650 μm of the central cornea was successfully re-imaged over the single 50-min observation. The images selected for analysis were overlapped by at least 25% of the fixed 400 × 400 μm frames obtained using this technique. The cell density in central cornea was typical for healthy patients, (12 ± 3 cells/mm^2). In each of the five sessions per visit, a mean of 63 ± 32 images were captured from the central cornea at the level of the sub-basal nerve plexus, between 45 and 55 μm depth from the corneal surface (Alzahrani et al., 2017; Colorado et al., 2019) (Fig. 1).

3.3. Image analysis

During each session, a region of interest of approximately 280 × 280 μm coverage was identified in five selected images in order to track a single cell. This area was selected from the total scanned area (650 × 650 μm), as shown in Fig. 2 A–E. Each frame contained a re-identified moving cell without visible dendrites (approximately 10 min apart over a 50-min period, including time zero) as well as re-identifiable static landmarks (main corneal nerve fiber junctions).

3.4. Time-lapse imaging of corneal DCs

Over the 50 min time-lapse period, a total of 12 individual cells were observed (Table 1). Nine cells without visible dendrites, three cells with visible dendrites and three stationary nerve junctions were identified, in the three separate eyes, and followed at each time-point. A total number of four cells per individual were included in the image analysis. During the observations, the cells without visible dendrites appeared to dynamically change location and size relative to the neighboring nerve landmarks, whereas cells with visible dendrites presented no movement as compared to control nerve junctions.

The average cell area of cells without visible dendrites and with visible dendrites was 42 ± 9 μm^2 and 80 ± 6 μm^2, respectively. Persistence (ratio) of the cells moving in one direction

from the start to the end position was observed in all cells without visible dendrites, indicating linear trajectory in the migratory path (0.84 ± 0.17) (Fig. 3). Cell movement was observed in the space between visible nerve fibres as well as crossing main nerve fibers and branches.

3.5. Cell displacement, trajectory and directional persistence speed

The three nerve junctions used in the analysis presented minimal variation over the five sessions in the three different corneas in displacement speed (0.05 ± 0.02 μm/min), trajectory path (0.14 ± 0.05 μm/min) and directional persistence (0.40 ± 0.02). Similar to the stationary nerve junctions, cells with visible dendrites were limited in movement with displacement speed (0.04 ± 0.01 μm/min), trajectory path (0.14 ± 0.02 μm/min) and directional persistence (0.29 ± 0.11). In contrast, the displacement trajectory and directional persistence speeds of corneal cells without visible dendrites (N = 9) was rapid and highly dynamic compared to cells with visible dendrites (N = 3). Displacement speed was 1.12 ± 0.21 μm/min. The trajectory (migratory path) speed was similar to displacement speed indicating a fairly linear path (1.35 ±0.17 μm/min). The cells showed a migration efficiency with a directional persistence ratio (displacement/trajectory) of 0.84 ± 0.17.

4. Discussion

This observational, quantitative study demonstrates for the first time corneal immune cell dynamics in healthy individuals. We showed that cells without visible dendrites moved rapidly at the sub-basal nerve plexus level and that cell movement is likely in three dimensions in the healthy corneal epithelial niche.

In animal studies (Zhao et al., 2003; Zhou and Petroll, 2010), corneal DCs have been describe as tridimensional structures with extending and retracting protrusions that move actively during wound healing as observed using three-dimensional time-lapse imaging in unstained cells (Zhou and Petroll, 2010). In humans, IVCM has been used for the quantification of corneal DCs with (Mastropasqua et al., 2006; Zhivov et al., 2005) and without cell dendrites (Marsovszky et al., 2013) in healthy and diseased cornea. The increased number of these cells in the central cornea has been used as clinical indicators of inflammatory conditions of the ocular surface (Lin et al., 2010). Interventional studies have also demonstrated changes in DC numbers in central cornea. However, the time frames used to measure this cell density is lapsed by hours (Alzahrani et al., 2016) weeks (Alzahrani et al., 2017) and years (Fagerholm et al., 2014). Given the results of this study, it would be reasonable to conclude that cells without visible dendrites are able to migrate to the central cornea at a significant high speed during both homeostasis and inflammatory conditions, and therefore cell density within the cornea could increase within minutes rather than hours or days apart.

IVCM has been used to study corneal nerve migration rate in healthy and diabetic conditions (Edwards et al., 2012), but has never been used before to create time-lapse image sequences of cellular movement in the living human cornea. The novel measure of immune cell dynamic has the potential to improve understanding of the inflammatory changes associated with ocular insult. However, its greatest potential may lie in its ability to quantify non-

invasively changes during inflammatory conditions such as systemic rheumatological diseases (Marsovszky et al., 2013; Villani et al., 2013), dry eye disease (Labbe et al., 2007; Lin et al., 2010), allergic responses (Hu et al., 2008; Villani et al., 2014), and drug induced toxicity (Liang et al., 2008). Another strength is the potential to study basic immunology and cellular responses to drug delivery and noxious stimuli.

There are technical challenges utilizing IVCM in human eyes. For example, the human eye makes small involuntary movements during ocular fixation and while the individual is breathing, therefore, obtaining good quality images and re-capturing those images at the same topographical location is difficult. Considering the 400 × 400 μm image area (160,000 μm^2) compared to the total size of the cornea (approximately 137 mm^2), the ability to identify and collect consecutive images from identical areas is technically challenging. Another challenge with the technique depends on the capability of participants to fixate on same point for a period of time while the other eye is being scanned (loss of fixation can occur due to visual accommodative issues). Another caveat of using this technique in humans is that laser exposure should not be over 45 min as safety measure suggested by manufacturer. This explains why we only followed the cells over 50 min with breaks of approximately 5–10 min between the observations of approximately 4 min long.

Despite these limitations, the identification of corneal nerve landmarks (nerve fiber junctions), at the sub-basal nerve plexus, as well as using an adequate instrument set up, well-positioned targets at each examination and clinical expertise in the acquisition of images can make the re-identification of a given location possible. The feasibility of successful re-imaging of the same corneal area has been demonstrated in this study in each of the five sessions lapsed by approximately 5–10 min in three individuals.

The cell somas of cells lacking visible dendrites, appeared to change in curvilinear shapes, moving across the focal plane in a X and Y direction. Fig. 2D shows how the tracked cells changed dramatically in size and shape, possibly due to Z displacement to either more superficial layers in the corneal epithelium or more posteriorly towards the underlying stroma. The Z migration is assumed by the change in cell area due to the cell leaving the plane of focus (Fig. 4).

Corneal DCs have been described as tridimensional structures with fast movement attributed to retractive protrusions (Metruccio et al., 2017; Ward et al., 2007; Zhao et al., 2003). As such, when using IVCM to image tridimensional structures, it is most likely that the changes in cell shape and size are a result of the two-dimensional focal plane and coronal view of the instrument capturing a different part of the cell as it migrates away from the plane of focus. Capturing Z movements by acquiring volume scans could potentially increase the accuracy of cell migration analysis, however the constant small movements by participants during image acquisition and the longer duration of collecting volume scans would reduce the capacity to collect the large number of sequence scans needed to track the same cells across time.

Bone marrow DCs from the stroma of bovine corneas move at a displacement speed (distance from start to end point) of around 0.18 μm/min and an average trajectory speed

(migratory path) of 0.83 μm/min (Zhao et al., 2003). In the present observational study, we found that human cells without visible dendrites, imaged in vivo, have a displacement speed of 1.12 μm/min, nearly five times faster than bone marrow-derived cells in ex vivo bovine corneas. These discrepancies in rates of movement could be explained by the capturing of these cellular dynamics in a living human compared to using cadaveric, ex vivo bovine corneas. Furthermore, another report of immune cell dynamics in limbal neovascularization induced by suture placement in mice, suggest that immune cell migration into stromal lymphatic vessels is around 9 μm/min (Steven et al., 2011). This indicates that immune cell migration in mice is faster in lymphatic vessels during injury compared to the healthy, avascular cornea in humans.

IVCM offers the advantage of live cell imaging of corneal structures and cellular processes in real time, and across time in patients. However, there are a number of limitations of in vivo imaging that can be difficult to avoid, especially when making inferences about immune cell subsets such as identifying their ontogeny, function or phenotype, all of which are now possible using extensive ex vivo analytical techniques such as single cell sequencing (Guilliams et al., 2016). One study has attempted to correlate IVCM images with ex vivo immunohistochemistry, to demonstrate the immunological phenotype of cells to confirm their identity as “dendritic cells” (Mayer et al., 2012). They provided evidence that the hyperreflective cells visible in vivo expressed the APC markers Langerin and HLA-DR (Mayer et al., 2012). However, it was not clear if the cells visible by IVCM were the same cells imaged ex vivo. It is clear that the precise identification of resident immune cells in human corneal epithelium, which are visible by IVCM, is an area in need of further investigation. Live cell imaging provides morphological identification and tissue location, and therefore most studies refer to these cells as dendritic cells with and without processes.

This novel study demonstrates that the displacement, trajectory and directional persistence speed of immune cells without visible dendrites was similar in three human corneas. Animal studies suggest that corneal DCs move faster in inflamed corneas (Seyed-Razavi et al., 2013). Using the methodology developed in this report, future studies could be done in eyes of patients with a range of local and systemic conditions that are known to cause DC activation in the central cornea (Jun et al., 2008;Schöllhorn et al., 2015; Shetty et al., 2016). Future studies using this novel approach should include a bigger scanned region in order to increase the number of cells tracked and also explore the potential differences between central and peripheral corneal cell behavior.

5. Conclusions

Despite the challenges of image acquisition in live individuals, the present study provides novel evidence of the feasibility to re-identify the same area and location over time by using corneal nerve landmarks in the sub-basal nerve plexus. Using this approach, this study demonstrated the migration and morphological alterations of cells without visible dendrites imaged over a 50-min period. This finding and technical approach could have implications for basic ophthalmic and immunology/cell biology research in human eyes and also serve as a gateway to investigate basic cellular immunology in a minimally invasive manner.

Supplementary Material

Refer to Web version on PubMed Central for supplementary material.

Acknowledgements

Acknowledgements to the participants who kindly volunteered for the study.

The authors alone are responsible for the content and writing of the manuscript.

Funding sources

This research did not receive any specific grant from funding agencies in the public, commercial, or not-for-profit sectors.

References

Al Rashah K, Pritchard N, Dehghani C, Ruggeri A, Guimaraes P, Russell A, Malik RA, Efron N, Edwards K, 2018 Corneal nerve migration rate in a healthy control population. Optom. Vis. Sci 95, 672–677. [PubMed: 30063664]

Alzahrani Y, Colorado LH, Pritchard N, Efron N, 2017 Longitudinal changes in Langerhans cell density of the cornea and conjunctiva in contact lens-induced dry eye. Clin. Exp. Optom 100, 33–40. [PubMed: 27353750]

Alzahrani Y, Pritchard N, Efron N, 2016 Changes in corneal Langerhans cell density during the first few hours of contact lens wear. Contact Lens Anterior Eye 39, 307–310. [PubMed: 26923921]

Beltman JB, Maree AF, de Boer RJ, 2009 Analysing immune cell migration. Nat. Rev. Immunol 9, 789–798. [PubMed: 19834485]

Choi EY, Kang HG, Lee CH, Yeo A, Noh HM, Gu N, Kim MJ, Song JS, Kim HC, Lee HK, 2017 Langerhans cells prevent subbasal nerve damage and upregulate neurotrophic factors in dry eye disease. PloS One 12, e0176153. [PubMed: 28441413]

Colorado LH, Markoulli M, Edwards K, 2019 The relationship between corneal dendritic cells, corneal nerve morphology and tear inflammatory mediators and neuropeptides in healthy individuals. Curr. Eye Res 44, 840–848. [PubMed: 30909745]

Cruzat A, Witkin D, Baniasadi N, Zheng L, Ciolino JB, Jurkunas UV, Chodosh J, Pavan-Langston D, Dana R, Hamrah P, 2011 Inflammation and the nervous system: the connection in the cornea in patients with infectious keratitis. Invest. Ophthalmol. Vis. Sci 52, 5136–5143. [PubMed: 21460259]

Edwards K, Pritchard N, Poole C, Dehghani C, Al Rashah K, Russell A, Malik RA, Efron N, 2016 Development of a novel technique to measure corneal nerve migration rate. Cornea 35, 700–705. [PubMed: 26938328]

Edwards K, Pritchard N, Vagenas D, Russell A, Malik RA, Efron N, 2012 Utility of corneal confocal microscopy for assessing mild diabetic neuropathy: baseline findings of the LANDMark study. Clin. Exp. Optom 95, 348–354. [PubMed: 22540156]

Efron N, 1998 Grading scales for contact lens complications. Ophthalmic Physiol. Optic 18, 182–186.

Fagerholm P, Lagali NS, Ong JA, Merrett K, Jackson WB, Polarek JW, Suuronen EJ, Liu Y, Brunette I, Griffith M, 2014 Stable corneal regeneration four years after implantation of a cell-free recombinant human collagen scaffold. Biomaterials 35, 2420–2427. [PubMed: 24374070]

Guilliams M, Dutertre CA, Scott CL, et al., 2016 Unsupervised high-dimensional analysis aligns dendritic cells across tissues and species. Immunity 45, 669–684. [PubMed: 27637149]

Hamrah P, Zhang Q, Liu Y, Dana MR, 2002 Novel characterization of MHC class II–negative population of resident corneal Langerhans cell–type dendritic cells. Invest. Ophthalmol. Vis. Sci 43, 639–646. [PubMed: 11867578]

Hu Y, Matsumoto Y, Adan ES, Dogru M, Fukagawa K, Tsubota K, Fujishima H, 2008 Corneal in vivo confocal scanning laser microscopy in patients with atopic keratoconjunctivitis. Ophthalmology 115, 2004–2012. [PubMed: 18584874]

Jun J, Bielory L, Raizman MB, 2008 Vernal conjunctivitis. Immunol. Allergy Clin 28, 59–82.

Labbe A, Brignole-Baudouin F, Baudouin C, 2007 [Ocular surface investigations in dry eye]. J. Fr. Ophtalmol 30, 76–97. [PubMed: 17287676]

Lee EJ, Rosenbaum JT, Planck SR, 2010 Epifluorescence intravital microscopy of murine corneal dendritic cells. Invest. Ophthalmol. Vis. Sci 51, 2101–2108. [PubMed: 20007837]

Liang H, Baudouin C, Pauly A, Brignole-Baudouin F, 2008 Conjunctival and corneal reactions in rabbits following short- and repeated exposure to preservative-free tafluprost, commercially available latanoprost and 0.02% benzalkonium chloride. Br. J. Ophthalmol 92, 1275–1282. [PubMed: 18723745]

Lin H, Li W, Dong N, Chen W, Liu J, Chen L, Yuan H, Geng Z, Liu Z, 2010 Changes in corneal epithelial layer inflammatory cells in aqueous tear-deficient dry eye. Invest. Ophthalmol. Vis. Sci 51, 122–128. [PubMed: 19628746]

Machetta F, Fea AM, Actis AG, de Sanctis U, Dalmasso P, Grignolo FM, 2014 In vivo confocal microscopic evaluation of corneal langerhans cells in dry eye patients. Open Ophthalmol. J 8, 51–59. [PubMed: 25317216]

Marsovszky L, Resch MD, Nemeth J, Toldi G, Medgyesi E, Kovacs L, Balog A, 2013 In vivo confocal microscopic evaluation of corneal Langerhans cell density, and distribution and evaluation of dry eye in rheumatoid arthritis. Innate Immun. 19, 348–354. [PubMed: 23204037]

Mastropasqua L, Nubile M, Lanzini M, Carpineto P, Ciancaglini M, Pannellini T, Di Nicola M, Dua HS, 2006 Epithelial dendritic cell distribution in normal and inflamed human cornea: in vivo confocal microscopy study. Am. J. Ophthalmol 142, 736–744 e732. [PubMed: 17056357]

Mayer WJ, Mackert MJ, Kranebitter N, Messmer EM, Grüterich M, Kampik A, Kook D, 2012 Distribution of antigen presenting cells in the human cornea: correlation of in vivo confocal microscopy and immunohistochemistry in different pathologic entities. Curr. Eye Res 37, 1012–1018. [PubMed: 22667765]

Metruccio MM, Tam C, Evans DJ, Xie AL, Stern ME, Fleiszig SM, 2017 Contributions of MyD88-dependent receptors and CD11c-positive cells to corneal epithelial barrier function against Pseudomonas aeruginosa. Sci. Rep 7, 1–14. [PubMed: 28127051]

Patel DV, McGhee CN, 2007 Contemporary in vivo confocal microscopy of the living human cornea using white light and laser scanning techniques: a major review. Clin. Exp. Ophthalmol 35, 71–88. [PubMed: 17300580]

Rosenberg ME, Tervo TM, Müller LJ, Moilanen JA, Vesaluoma MH, 2002 In vivo confocal microscopy after herpes keratitis. Cornea 21, 265–269. [PubMed: 11917174]

Schöllhorn L, Bock F, Cursiefen C, 2015 Thrombospondin-1 as a regulator of corneal inflammation and lymphangiogenesis: effects on dry eye disease and corneal graft immunology. J. Ocul. Pharmacol. Therapeut 31, 376–385.

Seyed-Razavi Y, Hickey MJ, Kuffova L, McMenamin PG, Chinnery HR, 2013 Membrane nanotubes in myeloid cells in the adult mouse cornea represent a novel mode of immune cell interaction. Immunol. Cell Biol 91, 89–95. [PubMed: 23146944]

Seyed-Razavi Y, Lopez MJ, Mantopoulos D, Zheng L, Massberg S, Sendra VG, Harris DL, Hamrah P, 2019 Kinetics of corneal leukocytes by intravital multiphoton microscopy. Faseb. J 33, 2199–2211. [PubMed: 30226811]

Shetty R, Sethu S, Deshmukh R, Deshpande K, Ghosh A, Agrawal A, Shroff R, 2016 Corneal dendritic cell density is associated with subbasal nerve plexus features, ocular surface disease index, and serum vitamin D in evaporative dry eye disease. BioMed Res. Int. 2016

Steven P, Bock F, Hüttmann G, Cursiefen C, 2011 Intravital two-photon microscopy of immune cell dynamics in corneal lymphatic vessels. PloS One 6, e26253. [PubMed: 22028842]

Su P-Y, Hu F-R, Chen Y-M, Han J-H, Chen W-L, 2006 Dendritiform cells found in central cornea by in-vivo confocal microscopy in a patient with mixed bacterial keratitis. Ocul. Immunol. Inflamm 14, 241–244. [PubMed: 16911987]

Tavakoli M, Hossain P, Malik RA, 2008 Clinical applications of corneal confocal microscopy. Clin. Ophthalmol 2, 435–445. [PubMed: 19668734]

Villani E, Baudouin C, Efron N, Hamrah P, Kojima T, Patel SV, Pflugfelder SC, Zhivov A, Dogru M, 2014 In vivo confocal microscopy of the ocular surface: from bench to bedside. Curr. Eye Res 39, 213–231. [PubMed: 24215436]

Villani E, Galimberti D, Del Papa N, Nucci P, Ratiglia R, 2013 Inflammation in dry eye associated with rheumatoid arthritis: cytokine and in vivo confocal microscopy study. Innate Immun. 19, 420–427. [PubMed: 23339928]

Ward BR, Jester JV, Nishibu A, Vishwanath M, Shalhevet D, Kumamoto T, Petroll WM, Cavanagh HD, Takashima A, 2007 Local thermal injury elicits immediate dynamic behavioural responses by corneal Langerhans cells. Immunology 120, 556–572. [PubMed: 17250587]

Williams KA, Coster DJ, 1997 Rethinking immunological privilege: implications for corneal and limbal stem cell transplantation. Mol. Med. Today 3, 495–501. [PubMed: 9430785]

Zhao M, Song B, Pu J, Forrester JV, McCAIG CD, 2003 Direct visualization of a stratified epithelium reveals that wounds heal by unified sliding of cell sheets. Faseb. J 17, 397–406. [PubMed: 12631579]

Zhivov A, Stave J, Vollmar B, Guthoff R, 2005 In vivo confocal microscopic evaluation of Langerhans cell density and distribution in the normal human corneal epithelium. Graefes Arch. Clin. Exp. Ophthalmol 243, 1056–1061. [PubMed: 15856272]

Zhou C, Petroll WM, 2010 Rho kinase regulation of fibroblast migratory mechanics in fibrillar collagen matrices. Cell. Mol. Bioeng 3, 76–83. [PubMed: 21132118]

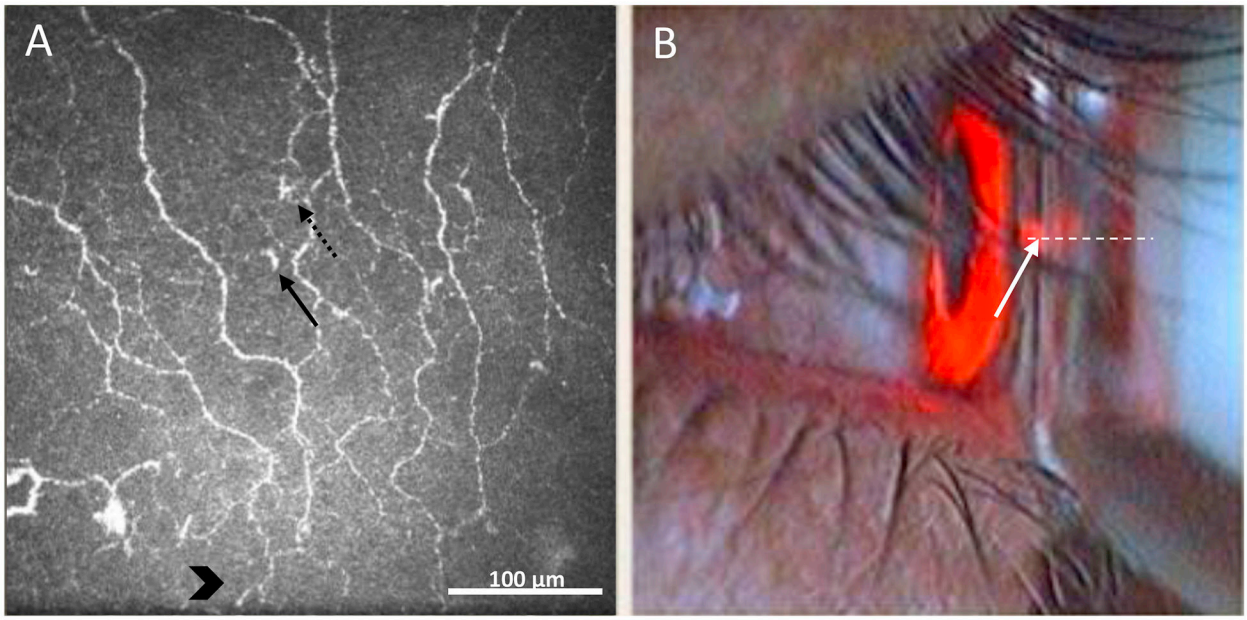

Fig. 1.

In vivo confocal microscopy viewing mode on the monitor during the acquisition of images. **A)** subbasal nerve plexus of the central cornea (400 × 400 µm^2). Dotted and solid arrows represent immune cells with and without visible dendrites, respectively. Chevron arrows indicate the location of nerve fibres immediately superior to the whorl of the sub-basal nerve plexus. **B)** Camera live image during image acquisition with guidance for alignment of the laser beam on the centre of the anterior corneal surface. Dotted line indicates the laser beam. The solid arrow shows the reflex of the laser beam on the central cornea.

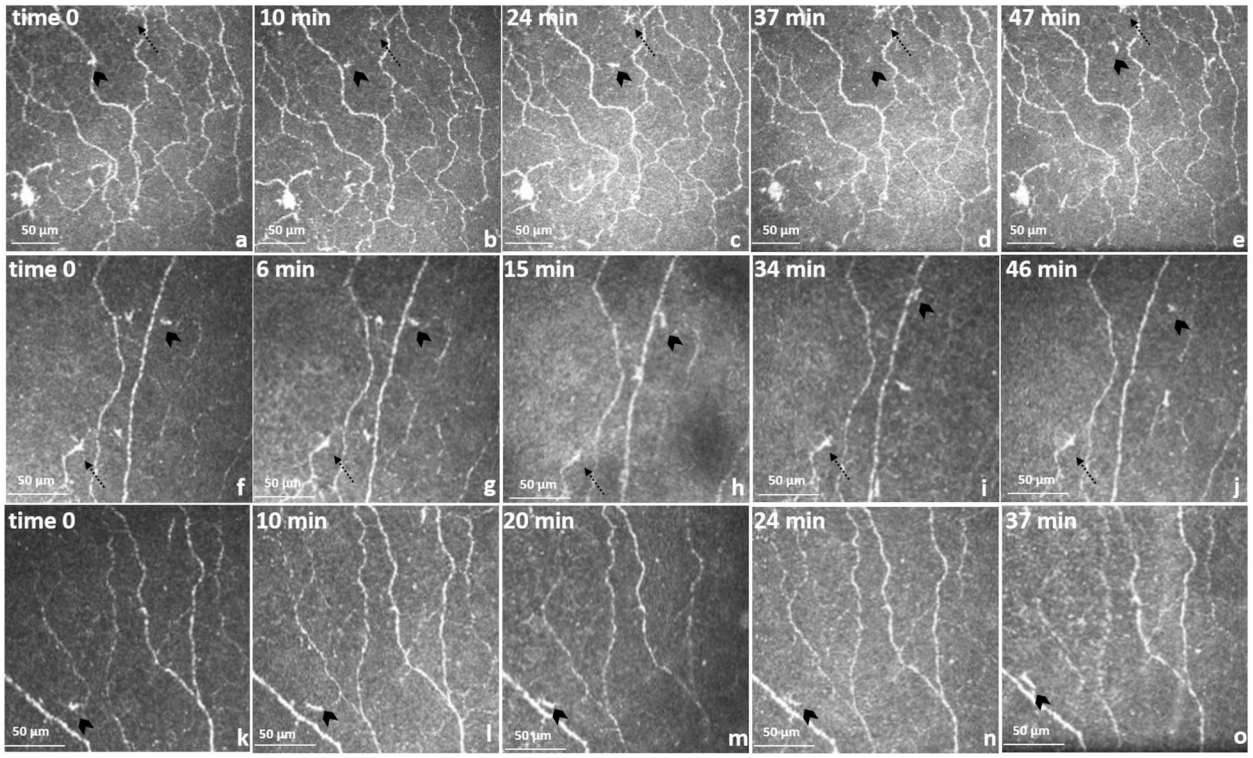

Fig. 2.

Cell movements in the sub-basal nerve plexus. Time sequence of optical section coronal view and trajectories of migratory cells. Migratory cells (cells without visible dendrites, chevron arrows) and static cells (defined cells with visible dendrites, doted arrows). **(a–e)** 41-year-old. Sequence of migratory cells (a) to (b) are moving crossing a main nerve fibre, therefore (a) appear to be part of the nerve. b,c,d,e shows a cell trajectory between nerve bundles. In image (d) cell changes dramatically in shape possibly due to Z movement. Area 280 × 280 µm. **(f–j)** 35-year-old and **(k–o)** 25-year-old. The area was reduced to 200 × 200 µm.

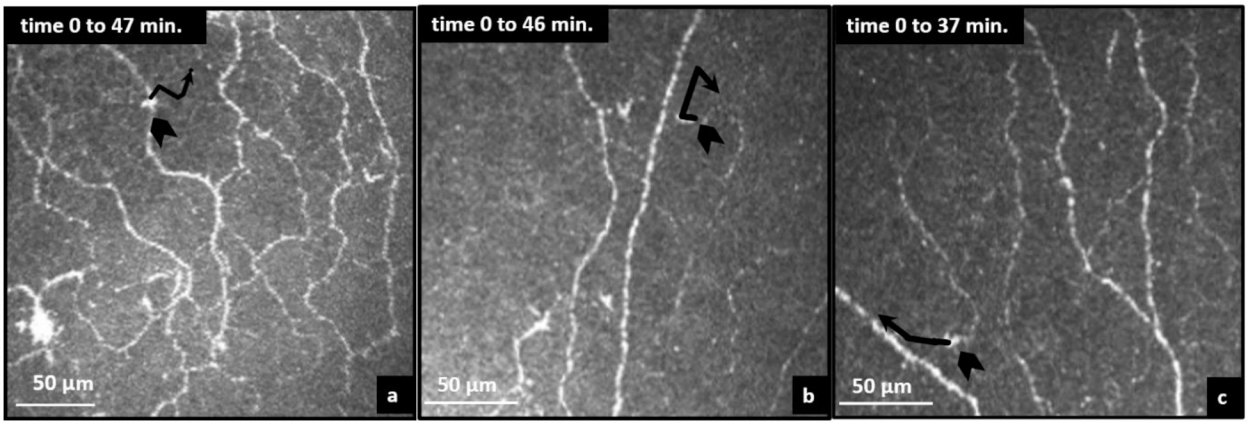

Fig. 3.

Cell trajectory paths. (a, b, c) cell trajectory showing a crossed way directional persistence for 41, 35 and 25-year-old participants, respectively.

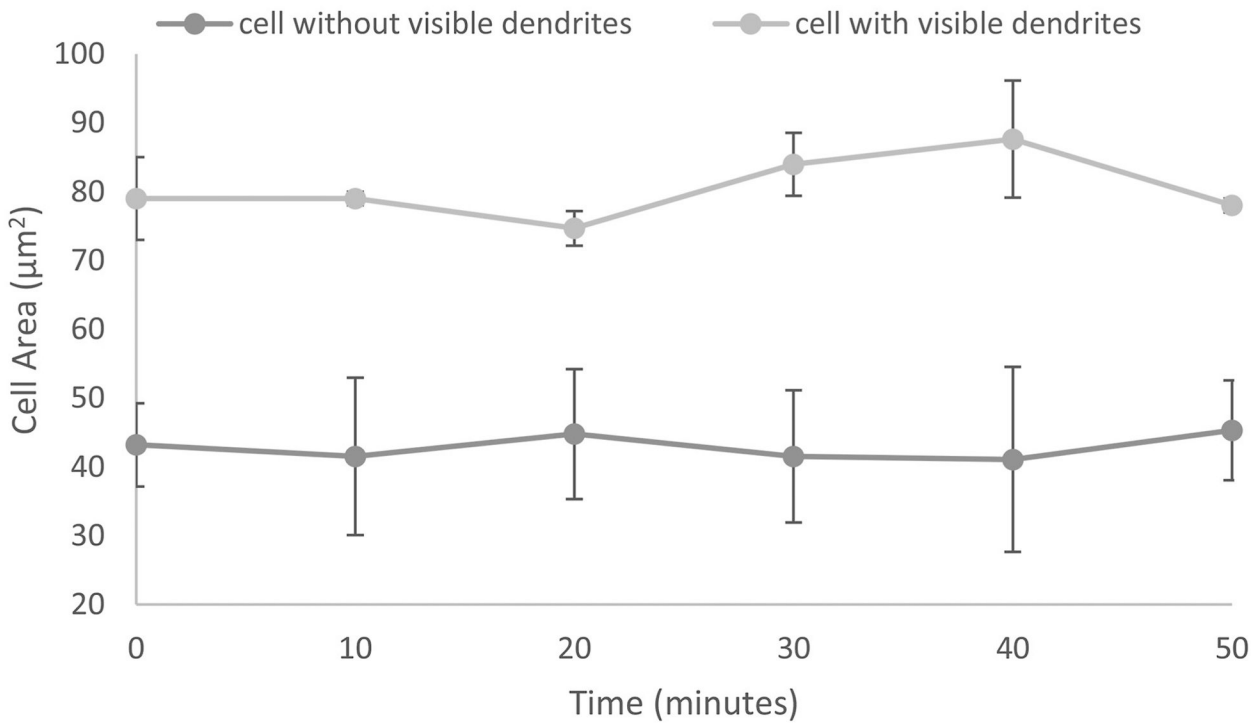

Fig. 4.

The cell areas of mature and immature dendritic cells was relatively stable over the imaging sessions.

Table 1

Dendritic cells size, displacement speed, trajectory path and persistence.

Participant and cell without visible dendrites	Cell size (μm^2)	Displacement speed (μm/min)	Trajectory Path (μm/min)	Persistence (ratio)	Track Length (μm)
Px 1 (41yo)					
cell 1	44 ± 12	0.8	1.4	0.5	53
cell 2	33 ± 10	1.3	1.5	0.9	55
cell 3	39 ± 10	1.0	1.1	1.0	51
Average	38 ± 10	1.0	1.3	0.8	53
with visible dendrites					
cell 4					
	80 ± 5	0.0	0.1	0.1	n.a
Px 2 (35 yo)					
cell 1	45 ± 4	1.0	1.4	0.7	48
cell 2	44 ± 10	1.2	1.4	0.9	50
cell 3	47 ± 4	1.4	1.4	1.0	49
Average	45 ± 2	1.1	1.4	0.8	49
with visible dendrites					
cell 4					
	80 ± 6	0.0	0.2	0.2	n.a
Px 3 (25 yo)					
cell 1	49 ± 8	1.0	1.3	0.8	52
cell 2	39 ± 12	1.1	1.4	0.8	51
cell 3	48 ± 6	1.0	1.2	0.8	52
Average	45 ± 5	1.0	1.3	0.8	52
with visible dendrites					
cell 4					
	82 ± 7	0.0	0.1	0.1	n.a